Generic Relaxation Spectra of Solid Polymers. I. Development of Spectral Distribution Model and Its Application to Stress Relaxation of Polypropylene

NABA K. DUTTA, GRAHAM H. EDWARD

Department of Materials Engineering, Monash University, Clayton, Victoria, Australia

Received 19 December 1996; accepted 16 January 1997

ABSTRACT: An important aspect of designing polymeric articles for engineering applications and predicting their properties over their lifetime is the computation of their time-dependent viscoelastic behavior. A simplified numerical computational technique based on a Gaussian spectral distribution model was developed to describe this behavior over a wide range of time and temperature. The model was used to describe the stress-relaxation behavior of isotactic polypropylene (iPP) over a wide range of strain, time, and temperature. It appears that a spectrum with two components (one distribution for the amorphous zone and the other for the crystalline zone) is sufficient to describe the viscoelastic behavior of iPP. The parameters specifying the distributions (mean relaxation time, standard deviation, and relaxation strength) may be obtained by nonlinear regression analysis and the temperature dependence of the distributions may be evaluated experimentally. An excellent fit between experimental data and the mathematical model is observed. The method may be applied generally for any linear viscoelastic property (e.g., static and dynamic relaxation and creep in tensile or shear) and for any polymer. © 1997 John Wiley & Sons, Inc. J Appl Polym Sci **66:** 1101–1115, 1997

INTRODUCTION

A precise knowledge of the mechanical behavior of polymeric materials used for engineering applications can be extremely important. However, the mechanical properties of polymeric solids depend strongly on time, temperature, loading procedure, and loading history.[1–3] To fully describe the mechanical properties of a material in a particular mode (e.g., tensile modulus), it is necessary to perform a set of experiments covering all of the time–temperature space practicable. These data can then be numerically or graphically collated and used as a description of the material. However, a number of complications arise: First, the results are dependent on the loading procedure, i.e., whether at constant strain, determining the stress-relaxation modulus; at constant stress, determining the creep modulus; or cyclic loading, determining the dynamic (or complex) modulus. It is not a satisfactory state to have a multiplicity of coefficients and functions, each fitting just one particular experiment for a particular material. Second, with numerical or graphical data, some method of interpolation (and possibly extrapolation) is often necessary, making use of the data inconvenient. In addition, the storage of large amounts of data is wasteful of both manpower and computer memory. For these reasons, it is generally more convenient and informative to describe a viscoelastic material in terms of a distribution function of time constants, where, in principle, one such distribution function is enough to completely characterize the material. This could be either the distribution of relaxation times or, alternatively, the distribution of retardation

Correspondence to: N. K. Dutta.

Contract grant sponsors: Australian Research Council (ARC); Moldflow Pty Ltd.

Journal of Applied Polymer Science, Vol. 66, 1101–1115 (1997)

 CCC 0021-8995/97/061101-15

times, more simply known as the relaxation spectrum or the retardation spectrum, respectively. The relaxation and retardation spectra are related to each other as an integral transform of each other at a particular temperature, although the analytical evaluation of these transforms is fraught with problems except in the simplest cases. Numerical evaluation of the transforms is another possibility, although a simple analytic spectrum is thus transformed to a numerical "reciprocal" spectrum. According to the linear theory of viscoelasticity, all time-dependent mechanical properties for a given substance under given experimental conditions can be correlated with each other through the rigorous mathematical relations involving the relaxation spectrum.[3–5]

The relaxation (or retardation) spectrum can be considered as a distribution function of relaxation (or retardation) times which, in the case of a thermorheologically simple material, remains unchanged with temperature and the viscoelastic response curves simply shift along the logarithmic time scale with temperature (toward a shorter time scale or higher frequencies with increasing temperature). In such a case, the time–temperature equivalence principle can be applied to describe the viscoelastic response of the material over a wide range of time, temperature, or frequency. Thermorheological simplicity demands that all the molecular mechanisms involved in the relaxation process have the same temperature dependence. However, it is recognized that the local polymer chain backbone motion and the motion of the different kinds of molecular moieties present in a polymer molecule exhibit different temperature dependencies, and in such a case, the distribution function changes form (shape) with changes in temperature and such thermorheologically complex materials are not reducible by simple superposition principles. The most thermorheologically simple material polyisobutylene (PIB) is thermorheologically complex. Recently, this point was discussed in detail by Plazek in his 1995 Bingham Medal address.[6]

Due to the versatility and importance of the relaxation spectrum, extensive research efforts have been made to obtain it from experimental data and theoretical models.[1–4] Different kinds of mathematical expressions have been used as distribution functions in the discussion of anelastic and dielectric behavior of materials,[3–5] and in most cases, they are complicated or cumbersome or no integral transform of the function is available. First-approximation procedures for evaluating the distribution function from graphical differentiation of experimental data on stress relaxation[1,7] and dynamic rigidity[8,9] or viscosity[10] have been used by many investigators. Ferry and Williams[11] developed a second-approximation method to derive the distribution spectrum of a viscoelastic material from experimental measurement. Andrews and Tobolsky[12] used a box distribution of relaxation times to approximate the relaxation behavior, but its usefulness was limited due to the fact that it could only successfully describe the longtime end of the relaxation time spectrum (and that for limited number of cases where the log time dependence of the modulus shows a straight-line relationship). Several investigators[13,14] have explored the possibility of constructing deformation maps, and this included modeling the time and temperature-dependent modulus of amorphous polymers, $E(t, T)$, under various loading conditions. They adapted and assembled the available constitutive equations for the different regimes (such as the glassy, viscoelastic, rubbery, viscous, and decomposition regimes) and used these to predict the behavior of the polymer materials over a wide time and temperature range.

It is generally accepted that no simple analytical or numerical method exists to correctly describe the viscoelastic behavior of polymeric solids. In this research program, an integrated research approach was undertaken to predict the viscoelastic response behavior of different polymeric materials over a wide range of time and temperature by using simple temperature-dependent distribution functions. A normal distribution of relaxation times was assumed to describe the individual relaxation processes of polymeric materials and the temperature dependence of each distribution was also considered. This method was used to describe the stress-relaxation behavior of isotactic polypropylene (iPP) over a wide range of temperature and time.

Polypropylene (PP) is a thermoplastic material of great commercial importance, especially for the injection-molding and fiber-spinning processes, due to its processing ease and the range of mechanical and performance characteristics. However, due to the existence of a variety of supermolecular structures including spherulites and multiple crystalline forms, it is a structurally complicated material. Many efforts have been made to construct a constitutive equation for PP. Kitagawa et al.[15] proposed a rate-dependent nonlinear constitutive equation based on Kremples'[16]

overstress model to explain and predict the behavior of PP in stress-relaxation, creep, and cyclic loading conditions. Many investigators[17–19] used simple three-element models to describe the viscoelastic behavior. In all these cases, experiments were carried out only at one or two particular temperatures and over a very limited period of time (1 s to a maximum of 1 day) and the models were used to explain the behavior in this narrow time/temperature frame. However, in case of polymeric solids, the relaxation and creep phenomena continue over a wide time scale (normally many decades) and are rapidly accelerated by small increases in temperature. Therefore, simple models are not adequate to describe the complex behavior of polymers like PP over the entire range of time and temperature space that may be encountered in practice.

THEORETICAL MODEL

The Stress-Relaxation Modulus

Phenomenologically, the stress-relaxation behavior of viscoelastic materials is most simply described as a Maxwellian relaxation (the model consists of an elastic element and a flow element in series), which predicts that the stress relaxes exponentially with time. The stress-relaxation modulus can be expressed by

$$E(t) = E_0 \exp - t/\tau \qquad (1)$$

where E_0 is the modulus of the elastic element; t, the time; and τ, the relaxation time of the material. When the time scale of observation is much shorter than τ, the material behaves as an elastic solid, whereas for any type of slow mechanical test, where the time scale is much larger than τ, the material will behave as a viscous liquid. However, for any observation of the intermediate time scale, where "t" is of the same order of magnitude as that of τ, both elasticity and flow will observed. Although the Maxwell model indicates the general nature of the polymeric behavior under stress, polymeric solids show rather more complex behavior.

A more realistic case can be modeled with a continuous set of Maxwell elements in parallel,[20] and the stress-relaxation modulus $E(t)$, a continuous decreasing function in increasing time, can be expressed as

$$E(t) = E_r + (E_u - E_r) \int_0^\infty g(\tau) \exp\left(-\frac{t}{\tau}\right) d\tau \qquad (2)$$

where $g(\tau)$ is the spectrum of relaxation times; E_u, the unrelaxed modulus; and E_r, the relaxed plateau modulus. $(E_u - E_r)$ is the time-dependent portion of the elastic modulus in a relaxation experiment. In the above equation, viscous mechanisms are ignored, and it is assumed that the viscoelastic solid relaxes from E_u to E_r.

In many respects, it is more convenient to describe the spectrum of relaxation times as a function of logarithmic time $(\ln \tau)$ rather than in terms of τ itself, in which case, eq. (2) can be expressed as

$$E(t) = E_r + (E_u - E_r) \times \int_{-\infty}^\infty h(\ln \tau) \exp\left(-\frac{t}{\tau}\right) d \ln \tau \qquad (3)$$

where $h(\ln \tau)$ is the spectrum of relaxation times expressed as a function of $(\ln \tau)$.

Both of the above distributions are normalized so that

$$\int_0^\infty g(\tau)\, d\tau = \int_{-\infty}^\infty h(\ln \tau)\, d \ln \tau = 1 \qquad (4)$$

If $h(\ln \tau)$ is specified for a particular temperature for all τ, then the stress-relaxation modulus is defined for this temperature, but the temperature dependence of the relaxations (and so the modulus) has also to be accounted for. In a thermorheologically complex material, the temperature dependence of the different relaxation processes known to occur in polymers[3,6] is different. Therefore, it is convenient at this stage to regard the overall distribution function $h(\ln \tau)$ as a sum of separate distributions describing the different relaxation processes. Using the usual convention that the relaxations are labeled, in turn, as α, β, γ, and δ, with decreasing temperature of occurrence at a particular time or frequency, the distribution function can be written as

$$h(\ln \tau) = h_\alpha(\ln \tau) + h_\beta(\ln \tau) + h_\gamma(\ln \tau) + \cdots = \sum_R h_R(\ln \tau), \qquad (5)$$

where $R = \alpha, \beta, \gamma, \delta$, etc., is the label for the particular relaxation. The α relaxation is gener-

ally due to the glass transition, but may be due to different mechanisms, particularly in semicrystalline polymers.

Substitution of eq. (5) in eq. (3) gives

$$E(t) = E_r + (E_u - E_r) \times \sum_R \int_{-\infty}^{\infty} h_R(\ln \tau) \exp\left(-\frac{t}{\tau}\right) d \ln \tau \quad (6)$$

Temperature Dependence of the Relaxations

The temperature dependence of the secondary relaxations (relaxations due to mechanisms other than the glass–rubber transition) can generally be described by an Arrhenius equation:

$$\ln a_T = \frac{\ln \tau_R}{\ln \tau_0} = \frac{Q_R}{R_0}\left(\frac{1}{T} - \frac{1}{T_0}\right) \quad (7)$$

where τ_R is the relaxation time at a particular temperature T; τ_0, the relaxation time at a reference temperature T_0; R_0, the gas constant; and Q_R, the activation energy in Joules/mole, and the subscript R represents α, β, γ, δ, as appropriate.

This transformation implies a particular shift of the relaxation spectrum $h_R(\log \tau)$, along the $\log \tau$ axis, with a different activation energy corresponding to each "R" describing the shift. The shape of each individual distribution on the $\log \tau$ scale will remain unchanged and the extent of the shift is given by the shift factor $\ln a_T$ in eq. (7). The α relaxation process of highly crystalline polymers will generally follow the Arrhenius equation. This is because in crystals unoccupied or free volume is quantized as vacancies of fixed volume.

On the other hand, in an amorphous polymer, the relaxation times describing the α relaxation usually follow the WLF equation[21]:

$$\ln a_T = \frac{\ln \tau_R}{\ln \tau_g} = -\frac{C_1(T - T_g)}{C_2 + (T - T_g)} \quad (8)$$

where $C_1 = 17.5$, $C_2 = 51.6$ K, T is the temperature at which the relaxation time is required, τ_R is this relaxation time, T_g is the glass transition temperature, and τ_g is the relaxation time at the glass transition temperature. If this temperature transformation of the relaxation times applies to all the times falling into the $R = \alpha$ term of eq. (5), this implies a shift of the relaxation spectrum $h_\alpha(\ln \tau)$ along the $\ln \tau$ axis, with no change of shape of the distribution.

The Distribution of Relaxation Times

Given that the temperature dependence of the relaxation times is described by either eqs. (7) or (8) as appropriate, to describe the modulus completely, the distribution $h(\tau)$ or its components $h_\alpha(\tau)$, $h_\beta(\tau)$ must be specified. This can be done either numerically or analytically, i.e., the distribution functions could be given as a table of values or as a mathematical function. These two possibilities will be illustrated in turn.

Numerical Description of the Relaxation Spectrum

A numerical description could give the value of the distribution functions at a necessarily large number of points, enabling the integral in eq. (6) to be numerically evaluated. Such a procedure would generally be cumbersome and wasteful of space in computations. If, however, instead of defining a continuous spectrum of relaxation times, the relaxation times are regarded as a finite set of discrete values, the individual relaxation spectra in eq. (5) could each be defined by a relatively small set of relaxation times.

For the glass transition ($R = \alpha$)-related relaxation times, these will be the relaxation times at T_g, whereas for the secondary relaxations, they will be the relaxation times at ∞, where the appropriate activation energy Q_R also has to be given. The individual discrete spectra can be expressed as follows:

$$h_R(\tau) = \sum_i \Delta h_{Ri} \delta(\tau - \tau_{Ri}) \quad (9)$$

where $\{\Delta h_{Ri}\}$ is the set of relaxation strengths; $\{\tau_{Ri}\}$ is the set of relaxation times whose elements for the α transition are determined from the set of relaxation times given at T_g using eq. (8) and for the secondary transitions ($R \neq \alpha$) are determined using eq. (7) and the set of relaxation times given at $T = \infty$; and δ is the delta function.

Substitution of eq. (9) in eq. (6) gives

$$E(t) = E_r + (E_u - E_r) \sum_R \sum_i \Delta h_{Ri} \exp\left(-\frac{t}{\tau_{Ri}}\right) \quad (10)$$

Note here that due to the normalization conditions [eq. (4)] the requirement on the discrete relaxation strengths is that

$$\sum_R \sum_i \Delta h_{Ri} = 1 \quad (11)$$

The quantity giving the relative strength of a particular relaxation is given by the sum of the Δh_{Ri} over i for a particular R.

Analytical Description of the Relaxation Spectrum

If, instead of numerically specifying the relaxation spectrum, an analytical form is assumed for the distributions, some potential economy of description is available. For example, it could be reasonably assumed that the distribution of relaxation times (in log time space) is Gaussian, so that

$$h_R(\ln \tau) = \frac{\Delta h_R}{\sqrt{2\pi}\,\Delta \ln_R} \exp\left[\frac{1}{2}\left(\frac{\ln \tau - \ln \tau_R}{\Delta \ln \tau_R}\right)^2\right] \quad (12)$$

where $\ln \tau_R$ is the mean value of the distribution; $\Delta \ln \tau_R$, the standard deviation; and Δh_R, the overall relative strength of the relaxation.

This distribution is completely defined by three parameters, and so only the mean, standard deviation, and relaxation strength need to be given for each individual relaxation. However, the simplification introduced is to some extent mitigated when the integral obtained by substituting eq. (12) into eq. (6) is considered. One means of obtaining a useful result is to make use of the Alfrey[1,22] approximation that approximates the exponential decay function to a step decay as follows:

$$\exp(-t/\tau) = 1 \quad \text{for } t \le \tau$$
$$= 0 \quad \text{for } t > \tau \quad (13)$$

Substitution of eqs. (12) and (13) in eq. (6) yields

$$E(t) = E_r + (E_u - E_r) \sum_R \int_{\ln t}^{\infty} \frac{\Delta h_R}{\sqrt{2\pi}\,\Delta \ln \tau_R} \times \exp\left[-\frac{1}{2}\left(\frac{\ln \tau - \ln \tau_R}{\Delta \ln \tau_R}\right)^2\right] d \ln \tau \quad (14)$$

This equation may be written more simply as

$$E(t) = E_r + (E_u - E_r) \sum_R \Delta h_R \times \int_U^{\infty} \frac{1}{\sqrt{2\pi}} \exp\left(\frac{-u^2}{2}\right) du \quad (15)$$

where $U = U(t) = (\ln t - \ln \tau_R)/\Delta \ln \tau_R$, and $u = (\ln \tau - \ln \tau_R)/\Delta \ln \tau_R$.

The integral in eq. (15) can be evaluated numerically using a simple published approximate formula[23] (details shown in the Appendix). The absolute error in estimation is less than 2.5×10^{-4}.

EXPERIMENTAL

Measurement Technique

A tensile stress relaxometer that records the stress and its decay has been developed for studying the effect of strain, temperature, and other variables on the long-term properties of polymers. One end of the test specimen is attached to the upper grip (stationary but adjustable) which is attached to a load cell. The load cell is connected to a PC through an ADC (PICOLOG, ADC 12, Pico Technology Limited, U.K.) which is used to record stress as a function of time. Picolog data logger software is used to collect measurements from the channel of the ADC and store them on a disk. The other end of the sample is attached to the lower grip that can be moved up and down over a range by a threaded screw. The sample is deflected to a preset deformation by a dead load. The elongation stop allows the imposition of any fixed elongation on the specimen. The grips and the sample are enclosed in a constant temperature air chamber. Elongation is measured by placing marks on the sample and determining the distance between the marks with a cathetometer. This method gives better accuracy than do strain gauges, particularly at higher temperature due to its noncontact nature. The variation in the results obtained by repetition of an experiment under identical conditions was less than 10%. Three samples were tested for each condition of strain and temperature and the average of these is reported.

Materials

The iPP used was SH 110, from Shell Australia, supplied as granules. The important properties

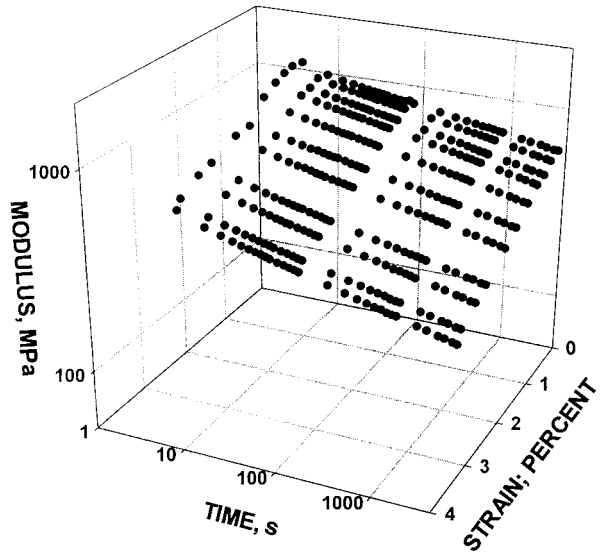

Figure 1 Effect of strain on modulus and its relaxation with time.

are density, 0.8983 gm/cc; specific heat, 2731.0 J/kg/deg; conductivity, 0.10 W/m/deg; melt density, 734.59 kg/cu; and viscosity at 225°C 392.29 and 93.09 Pa-s, respectively, at shear rates of 100 and 1000 s^{-1}.

Sample Preparation Technique

An end-gated two-plate mold of a cavity dimension 205 × 40 × 1.7 mm was used to mold rectangular plaques on an injection-molding machine. The molding parameters were melt temperature, 225°C; mold temperature, 40°C; injection time, 1.5 s; pack pressure, 60 MPa; pack time, 15 s; and cooling time, 20 s. For stress-relaxation measurements, 1.7 mm-thick strips of 180 × 10 mm were machined from the plaque with the long dimension along the mold-filling direction.

RESULTS AND DISCUSSION

Stress Relaxation as a Function of Strain

Figure 1 shows the tensile stress-relaxation characteristics of iPP at 30°C for different strains in the range of 0.3–4%. It is observed that linearity[24] (the stress-relaxation modulus curves are independent of the strain at which they are carried out) holds true for PP only at very low strains (<0.3%). However, the material appears to show generalized viscoelastic behavior, i.e., the effect of changing the strain at which stress relaxation occurs is merely to multiply the stress decay curve by a strain-dependent factor. There appears to be no substantial change in the shape of the decay curve over the range of strains and times investigated here. This can be expressed as

$$\frac{\sigma(t)}{\varepsilon} = E(t)\kappa(\varepsilon) \tag{16}$$

where $\kappa(\varepsilon)$ is the strain-dependent multiplication factor and is equal to 1 for small strains in the linear region. $\kappa(\varepsilon)$ was obtained by measuring the amount of vertical shift along the modulus scale necessary to make the curves superimpose. Values of κ are shown in Figure 2 where $\kappa = 1$ was chosen to correspond to 1% strain. Figure 3 shows a composite curve obtained by plotting the data from iPP as the reduced modulus. This shows that the behavior at any strain (within the experimental limit) and period of time can be predicted from the experimental curve at a particular strain over that period of time. This result is of great practical utility.

Stress Relaxation as a Function of Time and Temperature

Figure 4 shows a typical 3D plot of the tensile modulus as a function of time and temperature. Experiments were carried out over a temperature range of 22°C (295 K) to 157°C (430 K) and for times up to 4000 s. The modulus and time are plotted on log scales, and temperature, on a linear scale. The modulus decreases with increasing temperature as expected, and the shapes of the curves at various temperatures appear to be superimposable to form a single master relaxation curve, by shifting them horizontally along the log time axis. According to Ferry et al.,[10,21] the distribution of relaxation time at temperature T denoted by $G_T(t)$ is related to the distribution of relaxation times at a standard temperature by

$$\frac{\rho_0 T_0}{\rho T} G_T(a_T \tau) = G_{T_0}(\tau) \tag{17}$$

The quantity a_T is a function of temperature only and from eq. (17) is defined equal to unity at the reference temperature T_0. The quantity ρ_0/ρ are densities at T_0 and T, and for pure polymers, the ratio is quite a small correction factor that may be neglected within the accuracy of the theory. The correction factor T_0/T is small and was

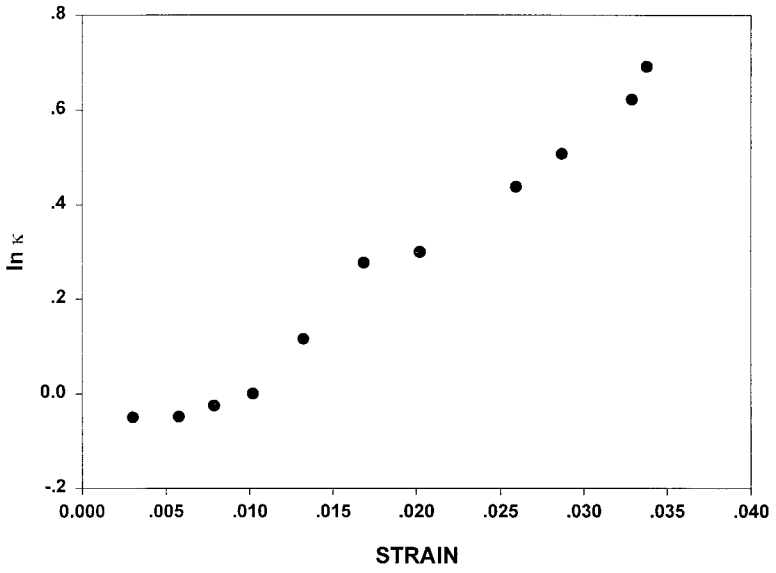

Figure 2 Plot of vertical shift, ln κ, as a function of strain.

introduced by Ferry[25] and Ferry et al.[21] to correct for the temperature effect resulting from entropy elasticity. However, Tobolsky and McLoughlin[26] indicated that its use is questionable from both a theoretical and experimental point of view. In our case, the composite relaxation curve does not show any better fit with the introduction of T_0/T and so the factor was omitted. Therefore, we have

$$G_T(a_T\tau) = G_{T_0}(\tau) \qquad (18)$$

The quantity a_T was obtained directly from the experimental relaxation curve at different temperatures plotted against logarithmic time by measuring the amount of shift along the time scale necessary to make these curves identical. A very careful test of eq. (18) was made for the stress-relaxation results obtained from iPP. It appears that the equation is sufficiently accurate in the range of 30 to 157°C. Figure 5 shows the master relaxation curve so obtained at a reference temperature of 30°C. To augment the results at low temperatures and short times, some data points extracted from published dynamic mechan-

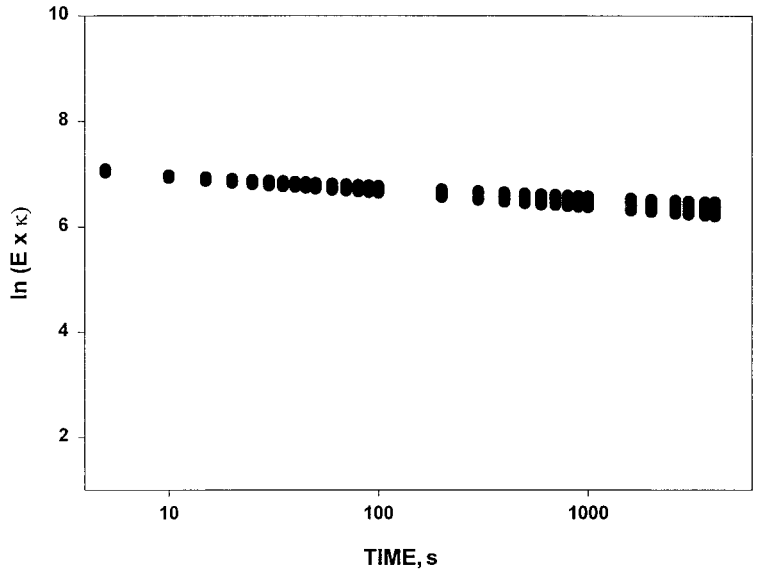

Figure 3 Composite graph for all different experimental strains.

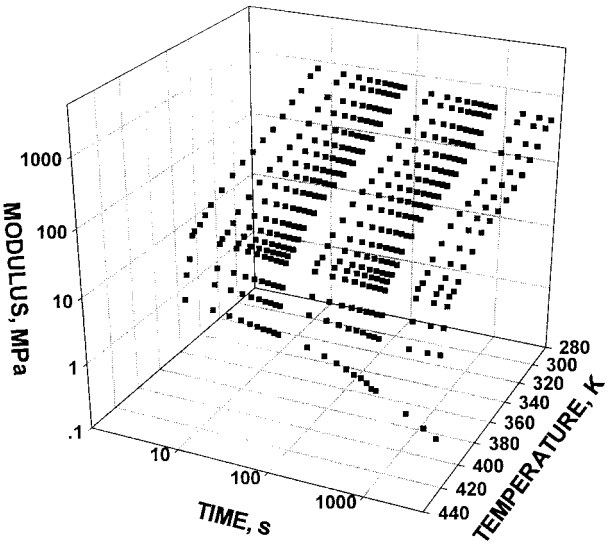

Figure 4 Plot of modulus as a function of time and temperature: 1.1% strain.

ical analysis (DMA) results on iPP (with proper conversion) were included.[27] Additionally, the stress-relaxation curve for the iPP over a very long period of time (280 h) is plotted in Figure 5. The short-time DMA results tally very well with the curve predicted by the reduced variable method, as do the real-time values over a long period of time. This gives further confidence in the experimental results and in the usefulness of the formulation.

Shift Factor and Apparent Activation Energy

The time dependence of the mechanical behavior of a linear viscoelastic material at constant temperature can be well represented by a relaxation spectrum, and the dependence on temperature is given by the shift factor a_T. Williams, Landel, and Ferry (WLF)[21] showed that the shift factor data for a number of amorphous polymer and glass-forming liquids can be described by the WLF eq. (8). Rearranging eq. (8), we can write

$$\frac{-(T - T_0)}{\log a_T} = \frac{C_2}{C_1} + \frac{(T - T_0)}{C_1} \qquad (19)$$

If the material data follow the WLF equation, then a plot of $-(T - T_0)/\log a_T$ versus $(T - T_0)$ should give a straight line, and from the slope and intercept, the values of C_1 and C_2 can be calculated. Figure 6 shows a plot of $-(T - T_0)/\log a_T$ vs. $(T - T_0)$ and it is clear that this is far from being a straight-line relationship, i.e., iPP does not conform to the WLF equation. This is not unexpected due to the fact that iPP is a semicrystal-

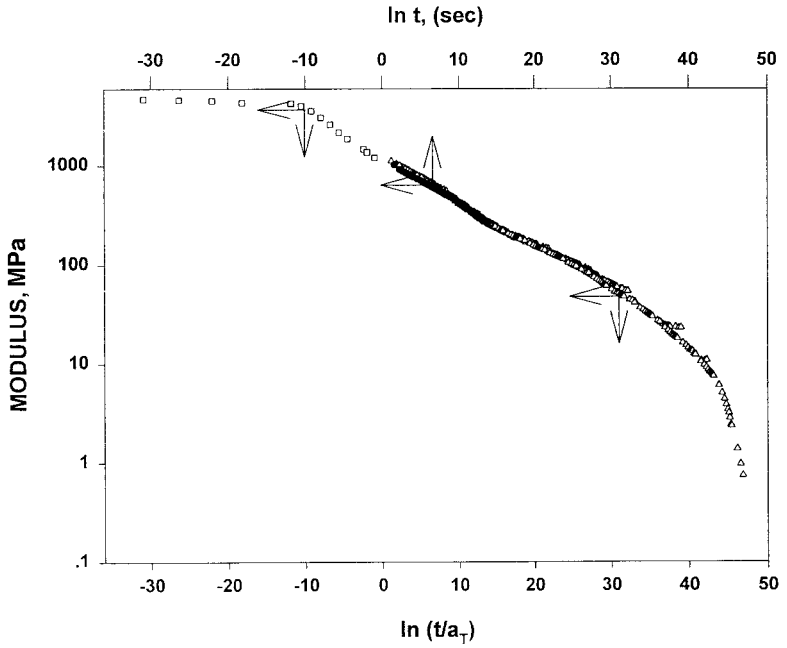

Figure 5 Master relaxation curve for PP reduced to 30°C. Decay of real-time modulus as a function of time is also compared with the master curve: (△) modulus versus $\ln(t/a_T)$; (●) modulus versus $\ln t$; (□) points taken from ref. 27.

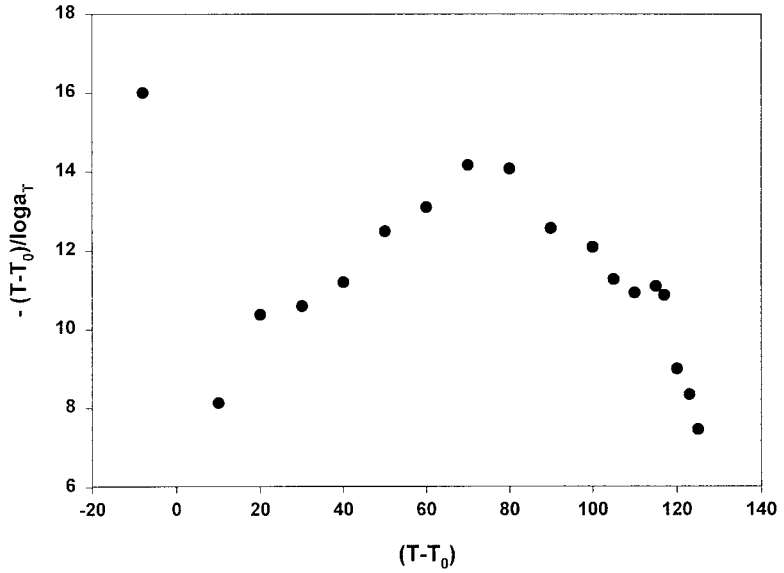

Figure 6 Plot of $-(T - T_0)/\log a_T$ versus $(T - T_0)$.

line polymer and its free volume can be thought to be quantized. Therefore, as discussed above, it is expected to follow the Arrhenius equation for the major relaxations.

The shift factors required to superpose data of Figure 5 are plotted against the inverse temperature in Figure 7. It appears that the data may be crudely described in terms of an activation energy Q defined by eq. (7). The sudden decrease in ln a_T above 150°C is caused by melting and the data points below this temperature may be roughly fitted to a straight line. The linear regression curve is also shown in the plot. The apparent activation energy was calculated from the slope of the regression curve and is 200 kJ/mol. This average activation energy is comparable with that of Attalla et al.[28] (163–221 kJ/mol depending on the experimental conditions), Faucher[29] (211 kJ/mol), and

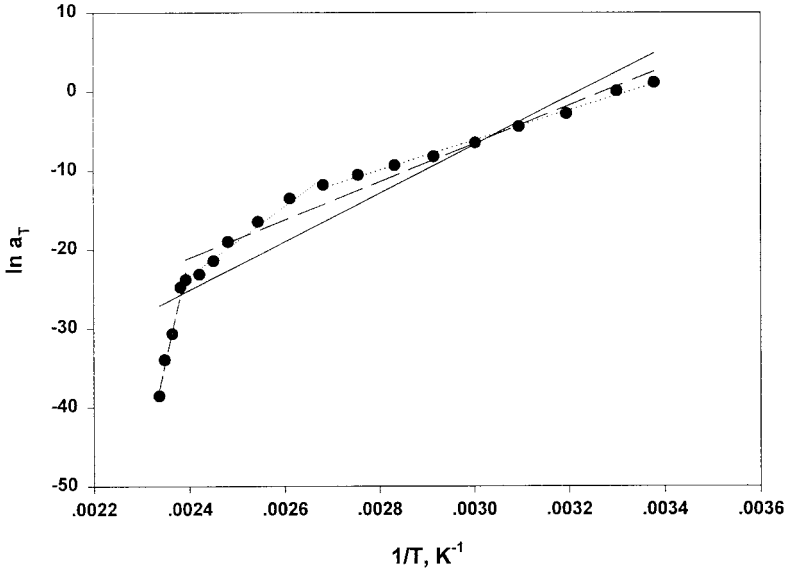

Figure 7 Shift factor versus inverse temperature plot: (——) first-order regression line considering one-component model; (----) first-order regression line considering two-component model; (· · · · · · ·) first-order regression line considering three-component model.

Wada[30] (167 kJ/mol). However, it is clearly seen from Figure 7 that a two-component fit could far better describe the relationship below 150°C. By using a two-component fit, the activation energies of the two corresponding relaxation processes are found to be 156 and 368 kJ/mol, respectively. iPP is a complex material with a complicated supermolecular structure and morphology[31] and a literature survey reveals that two or three main transitions (depending on material and testing method) are observed in iPP.[31–40] Dynamic mechanical analysis has always revealed two main transitions.[28,32,41] The highest temperature peak (α) in iPP is said to be associated with a crystalline phase-related relaxation (inter- or intracrystalline motion origin). This broad relaxation (lying from 40°C to higher than 100°C) is a complex mode hiding several loss processes.[38,39] The other transition (β) is the T_g, or the glass transition for iPP. Some investigators have observed two amorphous transitions in iPP with the characteristics of a glass transition (one from the amorphous zone restrained by the crystallites, the other from the relatively free amorphous zone).[41–43] The two activation energies obtained from Figure 7 considering the two-component model may be considered as the activation energies for the two relaxation processess, α and β, respectively. These activation energies were used for the nonlinear regression analysis as described in the following section by using eq. (15). It is important to note that Attalla et al.[28] observed experimentally that the activation energies for iPP were essentially independent of experimental strain. The variation in activation energy with different samples of different crystallinity and morphology was also found to be minimal.

Nonlinear Regression Analysis

A nonlinear regression analysis fitting eq. (15) to the experimental data at a strain of 1% was carried out by using the statistical software Sigmastat/Sigmaplot, Jandel Scientific Software, CA, U.S.A. The relaxation modulus, time, and temperature were used as variables, and the mean relaxation time ln τ_R, the standard deviation Δ ln τ, and the relative strengths Δh_R of the individual distributions were regarded as adjustable material parameters. E_r, E_u, Q, and T_0 were regarded as constants. The Sigmaplot/Sigmastat nonlinear regression uses the Marquardt–Levenberg algorithm[44–47] to find the coefficients (parameters) of the variables that give the best fit between the equation and the data. This algorithm seeks the values of the parameters that minimize the sum of the squared differences between the values of the observed and predicted values of the dependent variables by an iterative process. Sigmaplot/Sigmastat starts with initially provided parameters and proceeds to see how well the equation fits and then continues to make better guesses until convergence within a predefined tolerance is obtained. The nonlinear regression may be used to fit almost any equation desired.[47] First, a single distribution of relaxation times was considered. The parameters used for the single-relaxation nonlinear regression analysis were $\Delta h = 1$ (the relative strength of the relaxation) and $Q = 200$ kJ/mol (the activation energy calculated from linear regression). E_u was taken from the observed values for undrawn PP by Jarrigeon et al.[27] at low temperature and low frequency by dynamic mechanical analysis (with due conversion of the frequency scale to the time scale) as discussed above and shown in Figure 5. The Δ ln τ and ln τ_R were allowed to vary to get the best fit with the experimental results. The value of the response variable varies over a wide range with temperature and, therefore, the error variance is not uniform. Therefore, weighted nonlinear regression analysis was used, where the weight variable was defined as the reciprocal of the response variable. If this is not done, the total sum is sensitive mainly to the large response variable values, leading to a misleading nonlinear regression analysis.

The fitting of the calculated data with that of the experimental one is shown in Figure 8 in a 3D plot. The parameters necessary to have the best possible fit with the one-component normal distribution model are also shown in the figure. It is observed that the experimental and theoretical points appear to match excellently up to 80°C (within 10% accuracy) but the fit is poor above that temperature level. Particularly, in the temperature region of 90–130°C, the longer time section of the relaxation (the tail section) deviates significantly (the predicted value is much lower than the experimental one). The R^2 value calculated was 0.917 and indicates the poor quality of fitting. The R^2 value calculated here is defined[48] for nonlinear regression as

$$R^2 = 1 - \sum (Y - \hat{Y})^2 / \sum (Y - \bar{Y})^2$$

where Y is the response variable, $\hat{Y}$ is the fitted value of the response variable, and $\bar{Y}$ is the mean.

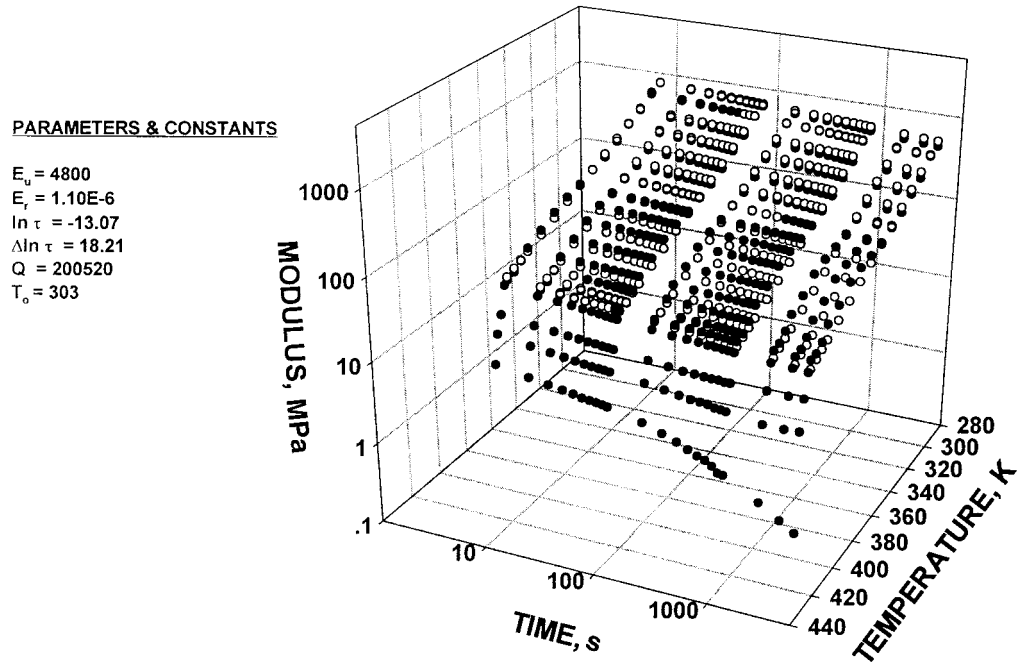

Figure 8 Fitting of experimental data with normal distribution function (one-component model): 1.1% strain: (●) experimental points; (○) theoretically calculated points.

Figure 9 shows the effect of temperature on the distribution of the relaxation time in the one-component model. With increasing temperature, the distribution shifts progressively toward the lower time scale; however, the shape of the distribution remains unchanged, i.e., the behavior of a thermorheologically simple material. Figure 10 depicts the calculated modulus over a wide range of time and temperature. The one-component model can predict, satisfactorily, the modulus values in the intermediate range of time and temperature. At low temperature and/or shorter time

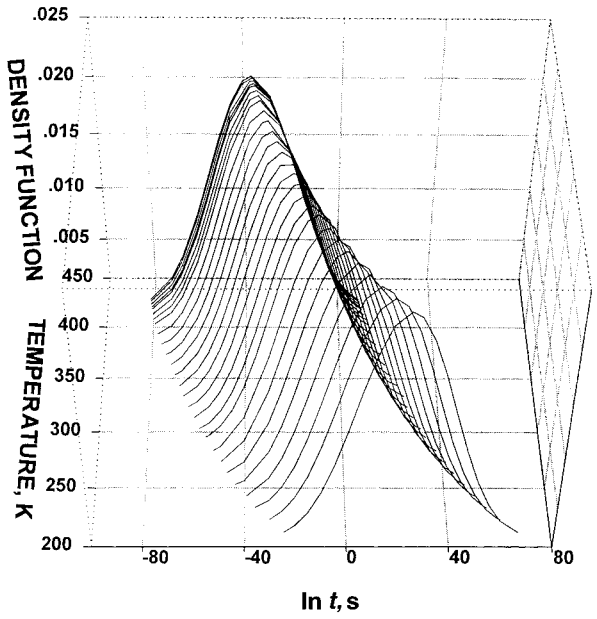

Figure 9 Effect of temperature on the distribution of the relaxation time (one-component model).

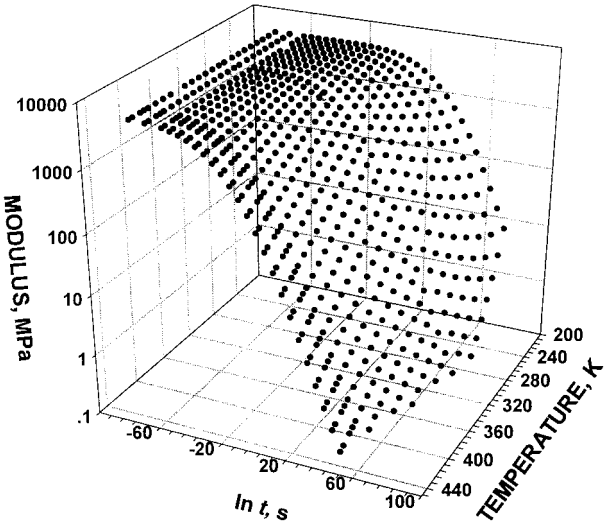

Figure 10 Theoretically calculated modulus over a wide range of time and temperature using one-component normal distribution model.

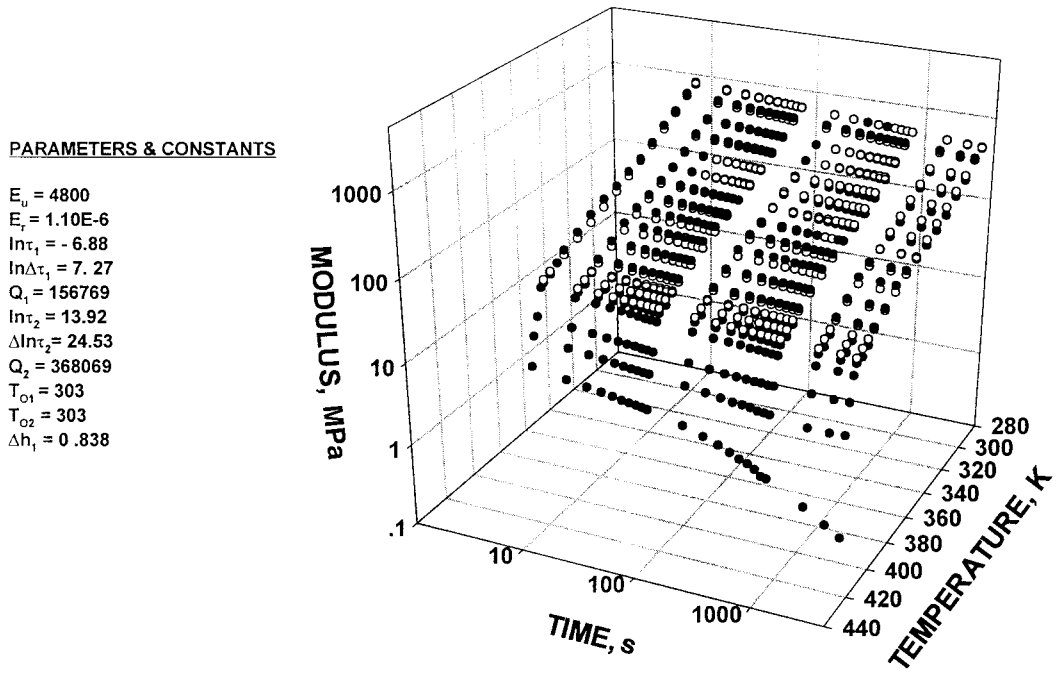

Figure 11 Fitting of experimental data with normal distribution function (two-component model): 1.1% strain: (●) experimental points; (○) calculated points.

and higher temperature and/or longer time, the predicted values are significantly lower than the experimental ones. Therefore, it appears that iPP is a thermorheologically complex material and a one-component normal distribution model is not sufficient enough to describe the linear viscoelastic behavior.

To improve on the one-relaxation fit, a two-component normal distribution model was considered for the fitting procedure. In this case, Q_1 and Q_2 obtained from Figure 7 were used. The relative strength of the distributions is Δh in one case and $(1 - \Delta h)$ in the other (because the total strength is 1). The fitting of the calculated surface to the experimental data is shown in Figure 11, where a weighted regression method was also employed. The parameters necessary to achieve the fit are also shown in the graph. As observed in the figure, an excellent fit is apparent over the whole range of temperature. However, above 150°C (where melting of crystallites takes place), an error of more than 25% was observed (the predicted values are much higher than the experimental one). The effect of temperature on the two distributions is illustrated in Figure 12. The individually normalized distribution curves for both the distributions are shown. The actual overall distribution will be the sum of the relative strengths of the two distributions [Δh component 1 + $(1 - \Delta h)$ component 2]. The second component that has about a 16% contribution to the process is broader compared to that of the first one. This distribution may be attributed to the crystalline phase-related relaxation, whereas the first component is related

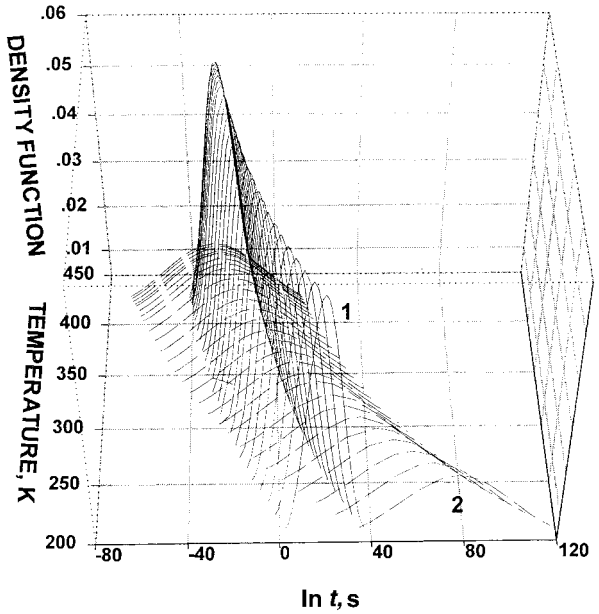

Figure 12 Effect of temperature on the distribution of the relaxation times (two-component model): (——) component 1; (------) component 2.

to the amorphous phase of iPP. Because the activation energies of the two relaxation processes are different, their shift in position with temperature is different, and so the shape of the overall distribution also changes with temperature, which is clearly observed in Figure 12, i.e., the thermorheological complexity of the polymeric material like iPP may be addressed by assuming that the material has two or more different relaxation distributions, each of which is thermorheologically simple but have different temperature dependencies. The predicted modulus over a wide range of time and temperature using the two-component normal distribution model is illustrated in Figure 13, and it can be seen that the two-component model can predict the modulus accurately from very low to high temperatures.

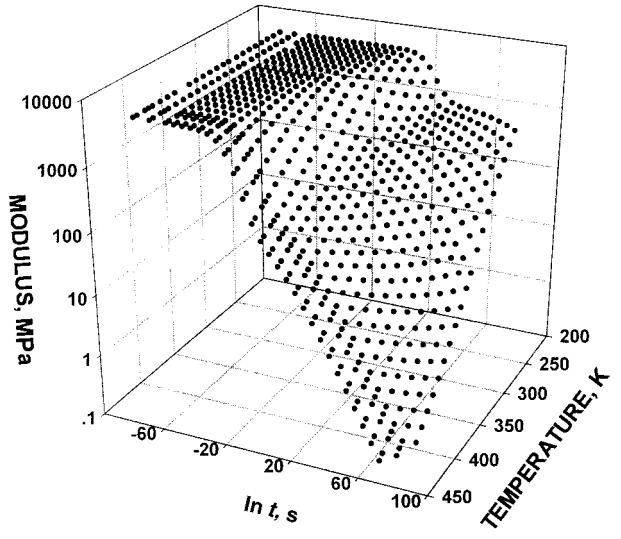

Figure 13 Theoretically calculated modulus over a wide range of time and temperature using two-component normal distribution model.

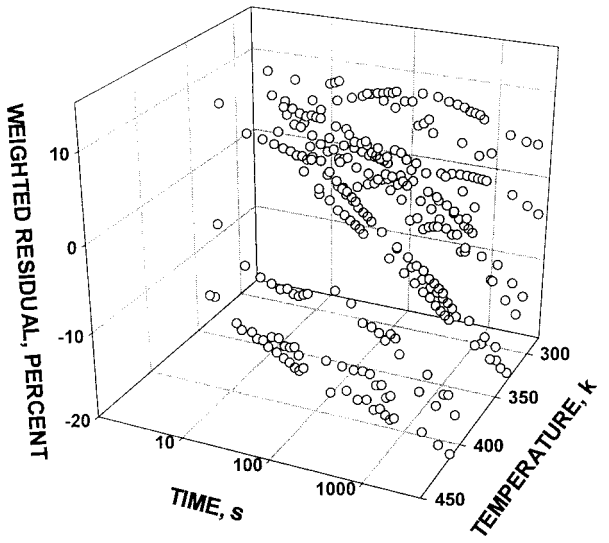

Figure 14 Plot of the residuals for the two-component regression of iPP.

Determining Model Adequacy

Figure 14 shows the plot of weighted residual percent (residual/response variable $\times$ 100) against the explanatory variables, time and temperature, and the residual varies between +10 and −15%. Although the residual is low, the pattern of the plot is not an ideal unstructured horizontal band centered at zero. The systematically decreasing structural band indicates the faster decay of the experimental points compared to the response variable, and it seems that a further very weak relaxation process would need to be included to model the data with increased accuracy. However, three-component fitting makes the computation significantly more complicated and time-consuming. The R^2 value for the two-component fit is 0.994, which clearly indicates the excellent quality of fitting and leaves little room for further improvement. To build confidence in the parameters, several regression analyses were carried out using starting values for the various parameters far away from the known final values. Convergence was always observed to the reported parameters, giving increased confidence regarding the final parameters obtained and that the location of the absolute minimum was found.

Regression analysis assumes normality of the underlying population or residuals of the response variables and can become unreliable if this assumption is violated. Sigmastat software was used for normality testing, which uses the Kolmogorov–Smirnov (with Lilliefors' correction) procedure[49] to test normality of the estimated underlying population. The Kolmogorov–Smirnov procedure tests the null hypothesis

$$H_0 : F_n(x) = F_0(x)$$

against the alternative

$$H_a : F_n(x) \neq F_0(x)$$

where $F_0(x)$ and $F_n(x)$ are, respectively, the continuous cumulative distribution function (cdf) of the hypothesized distribution and the sample distribution. The Kolmogorov–Smirnov test statistic

D_n is given by the maximum absolute difference between the sample cdf and the cdf of the hypothesized distribution, written as

$$D_n = \max|F_n(x) - F_0(x)|$$

When the hypothesis that $F_n(x) = F_0(x)$ is true, D_n has a distribution which is independent of $F_0(x)$. This distribution of D_n was tabulated[50] as a function of n and α (level of significance) when $F(x) = F_0(x)$. The hypothesis that $F(x) = F_0(x)$ is rejected at the α level of significance whenever $D_n(x) > d_{\alpha;n}$, where $d_{\alpha;n}$ are the values given in the table of Kolmogorov–Smirnov test statistics. The residual observed in this experiment is nonuniform and the standardized residual was used for the hypothesis testing. The details of the calculation of the standardized residual are discussed elsewhere[51] and it is emphasized that for checking the normality assumption one must use the standardized residual. The standardized residual at the 10 s data point from each experimental temperature was used for the calculation (at a particular temperature, all the remaining points are scaled by and so associated with the first data point in the relaxation testing). In the testing of the data, a 5% level of significance was used, and the critical value for $d_{0.05;15} = 0.338$ is obtained from the table.[50] By using the Sigmastat, the D_n value obtained for the population is 0.109 with a P value of 0.788. Thus, the hypothesis that $F(x)$ is normally distributed is accepted.

By using the two-component model, the modulus of iPP at any desired time and temperature can be calculated rapidly and precisely. As mentioned earlier, Attalla et al.[28] found that the activation energy values of the relaxations are essentially independent of the strain for iPP. Therefore, if the material shows generalized viscoelastic behavior (as iPP does, as discussed earlier), the behavior at any strain (within some limit) and over any period of time can be predicted from the calculated modulus at some other strain over that period of time. This is of great experimental and computational convenience. To allow greater application of the simple model, different polymers of different structure, crystallinities, and morphology are under investigation.

The authors would like to express their appreciation to the Australian Research Council (ARC) and to Moldflow Pty Ltd. for financial support. The authors also wish to thank Moldflow Pty. Ltd. for supplying the material data. Valuable discussion with R. Zheng and P. Kennedy of Moldflow Pty. Ltd. and Ajit Majumder of the Department of Econometrics, Monash University, are gratefully acknowledged. The authors also express their sincere gratitude to one of the referees for his constructive criticism.

APPENDIX: NUMERICAL APPROXIMATION TO THE CONTINUOUS CUMULATIVE DISTRIBUTION[23]

If

$$I(U) = \frac{1}{\sqrt{2\pi}} \int_U^\infty \exp\left(\frac{-u^2}{2}\right) du$$

then for $U > 0$, $I(U) = 1 - P(U) = 1 - P(|U|)$, and for $U < 0$, $I(U) = P(-U) = P(|U|)$, where $P(|U|) = 1 - \frac{1}{2}(1 + c_1U + c_2U^2 + c_3U^3 + c_4U^4)^{-4} + \varepsilon(U)$, where $c_1 = 0.196854$, $c_2 = 0.115194$, $c_3 = 0.000344$, $c_4 = 0.019527$, and $|\varepsilon(U)| < 2.5 \times 10^{-4}$.

REFERENCES

1. T. Alfrey, *Mechanical Behaviour of High Polymers,* Interscience, New York, 1948.
2. A. V. Tobolsky, *Properties and Structure of Polymers,* Wiley, New York, 1960.
3. N. G. McCrum, B. E. Read, and G. Williams, *Anelastic and Dielectric Effects in Polymeric Solids,* Wiley, New York, 1967.
4. J. D. Ferry, *Visco Elastic Properties of Polymer;* 2nd ed., Wiley, New York, 1970.
5. B. Gross, *Mathematical Structure of the Theories of Viscoelasticity,* Hermann, Paris, 1953.
6. D. J. Plazek, *J. Rheol.,* **40**(6), 987 (1996).
7. T. Alfrey and P. Doty, *J. Appl. Phys.,* **16,** 700 (1945).
8. A. W. Nolle, *J. Polym. Sci.,* **5,** 1 (1950).
9. R. D. Andrews, *Ind. Eng. Chem.,* **44,** 707 (1952).
10. J. D. Ferry, W. M. Sawyer, G. V. Browning, and A. H. Groth, Jr., *J. Appl. Phys.,* **21,** 513 (1950).
11. J. D. Ferry and M. L. Williams, *J. Colloid Sci.,* **7,** 347 (1952).
12. R. D. Andrews and A. V. Tobolsky, *J. Polym. Sci.,* **7,** 221 (1951).
13. D. G. Gilbert, M. F. Ashby, and P. W. R. Beaumont, *J. Mater. Sci.,* **21,** 3194 (1996).
14. G. H. Edward and R. M. Glen, *Mater. Forum,* **11,** 117 (1988).
15. M. Kitagawa, T. Mori, and T. Matsutani, *J. Polym. Sci. Part B Polym. Phys.,* **27,** 85 (1989).
16. E. Kremples, *Trans. ASME J. Eng. Mater. Tech.,* **101,** 380 (1979).

17. T. Ariyama, *Polym. Eng. Sci.,* **33,** 18 (1993).
18. T. Ariyama, *Polym. Eng. Sci.,* **33,** 1494 (1993).
19. F. Daver and B. W. Cherry, *J. Appl. Polym. Sci.,* **59,** 453 (1996).
20. E. Wiechert, *Wied. Ann. Phys.,* **50,** 335, 546 (1893).
21. M. L. Williams, M. L. Landel, and J. D. Ferry, *J. Am. Chem. Soc.,* **77,** 3701 (1955).
22. T. Alfrey and P. Doty, *J. Appl. Phys.,* **16,** 700 (1945).
23. M. Abramowitz and I. A. Stegun, Eds., *Handbook of Mathematical Functions with Formulas, Graphs, and Mathematical Tables,* Applied Mathematics Series, National Bureau of Standards, Washington, DC, 1964, p. 931.
24. L. Boltzmann, *Prog. Ann. Phys.,* **7,** 624 (1876).
25. J. D. Ferry, *J. Am. Chem. Soc.,* **72,** 3746 (1950).
26. A. V. Tobolsky and J. R. McLoughlin, *J. Polym. Sci.,* **8,** 543 (1954).
27. M. Jarrigeon, B. Chabert, D. Chatain, C. Lacabanne, and G. Nemoz, *J. Macromol. Sci.—Phys. B,* **17**(1), 1 (1980).
28. G. Attalla, I. B. Guanella, and R. E. Cohen, *Polym. Eng. Sci.,* **23,** 883 (1983).
29. J. A. Faucher, *Trans. Soc. Rheol.,* **3,** 81 (1959).
30. Y. Wada, *J. Phys. Soc. Jpn.,* **16,** 1226 (1961).
31. J. Krager-Kocsis, Ed., *Propylene—Structure, Blends and Composites. Vol 1, Structure and Morphology,* Chapman & Hall, London, 1995.
32. N. G. McCrum, *Makromol. Chem.,* **34,** 65 (1959).
33. R. L. Miller, *Polymer,* **1,** 135 (1960).
34. N. G. McCrum, *J. Polym. Sci. B,* **2,** 495 (1964).
35. S. S. Turley and H. Keskkula, *J. Appl. Polym. Sci.,* **92,** 693 (1965).
36. J. M. Crissman, *J. Polym. Sci. C,* **23,** 583 (1968).
37. A. J. Owen and I. M. Ward, *J. Macromol. Sci.—Phys. B,* **7,** 417 (1973).
38. E. J. Parry and D. Tabor, *Polymer,* **14,** 617 (1973).
39. I. Inamura, H. Ochiai, and H. Yamamura, *J. Polym. Sci. Polym. Phys. Ed.,* **12,** 2267 (1974); **14,** 1221 (1976).
40. M. Fujiyama and T. Wakino, *J. Appl. Polym. Sci.,* **35,** 29 (1988).
41. D. L. Beck, A. A. Hiltz, and J. R. Knox, *SPE Trans.,* **3,** 279 (1963).
42. Y. Wada, Y. Hotta, and R. Suzuki, *J. Polym. Sci. C,* **23,** 583 (1968).
43. R. F. Boyer, *J. Macromol. Sci.—Phys. B,* **8,** 503 (1973).
44. W. H. Press, B. P. Flannery, S. A. Teukolsky, and W. T. Vetterling, *Numerical Recipes,* Cambridge University Press, Cambridge, 1986.
45. J. C. Nash, *Compact Numerical Methods for Computers: Linear Algebra and Functional Minimization,* Wiley, New York, 1979.
46. D. W. Marquardt, *J. Soc. Ind. Appl. Math.,* **11,** 431 (1963).
47. *Transform and Nonlinear Regressions for Windows—Users Manual,* Jandel Scientific Software, San Rafael, CA, 1995.
48. T. O. Kvalseth, *Am. Stat.,* **39,** 279 (1985).
49. *SigmaStat User's Manual,* Jandel Scientific Software, San Rafael, CA, 1996.
50. A. L. Bowker and G. J. Lieberman, *Engineering Statistics,* Prentice-Hall, Englewood Cliffs, NJ, 1972, p. 456.
51. T. P. Ryan, *Modern Regression Methods,* Wiley, New York, 1996.